

# Influence of the stereo-EEG sensors setup and of the averaging on the dipole localization problem

Steven Le Cam<sup>1</sup>, Vairis Caune<sup>1</sup>, Radu Ranta<sup>1</sup>, Louis Maillard<sup>1,2</sup>, Laurent Koessler<sup>1</sup> and Valérie Louis-Dorr<sup>1</sup>

**Abstract**— While scalp EEG/MEG source imaging have been extensively studied in the last two decades, the case of source localization from invasive measurements has resulted in few works to date. Yet there is a lot to gain from stereo-electroencephalographic (SEEG) recordings, providing high signal to noise ratio measurements of the explored brain structures. The SEEG setup consists in multi-contact electrodes inserted in the brain volume, each containing a dozen of collinear measuring contacts. This particular setup raises the question of the conditioning of the inverse problem. In recent works, we have evaluated the feasibility to localize a single dominant equivalent dipole facing different sensors and noise configurations. We deepen here the analysis by evaluating the influence of the chosen subset of sensors and of the number of averaged time samples on the accuracy of the localization. We conduct experiments on simulated data as well as on real epileptic spikes, illustrating the trade off to be made between these two factors.

**Index Terms**— EEG, Stereo-electroencephalography (SEEG), Dipolar Localization, Inverse problem, Epileptic spikes

## I. INTRODUCTION

In clinical context, stereo-electroencephalography (SEEG) is used for exploring targeted structures assumed to be responsible for the epileptic events. Generally, the SEEG signals are observed using a bipolar montage, offering a local vision of the activity in the close neighborhood of the contacts. If the *priors* guiding the placement of the intracranial electrodes are valid and the number of inserted electrodes is high enough, this evaluation indeed allows a precise delineation of the epileptogenic zone [1]. However, a misplacement of the electrodes or a too sparse spatial sampling might induce imprecisions in the identification of the pathological structures. By using the raw SEEG recordings, the propagated potential field of the sources is preserved, making it possible to identify brain generators not necessarily in the close neighborhood of the electrodes. Besides, SEEG are less affected by electromagnetic noise or by extra-cerebral artifacts constantly polluting the scalp measurements, and are thus a promising tool for localizing accurately deep sources in the explored structures.

The EEG inverse problem has been extensively studied [2], [3], [4], while intracranial measurements have been restricted for validation purposes [1]. Few studies on the inverse problem based on invasive measurements can be found

in the literature. Yvert *et al.* [5] developed a distributed source imaging approach for source localization of temporal auditory areas, using electrocorticographic recordings. Chang *et al.* [6] evaluated dipole source estimation from SEEG, based on simulated data. Still on simulations, Ellenrieder *et al.* [7] addressed the intracranial forward modeling problem using a similar dipole inversion procedure.

In recent works, we studied the SEEG-based dipole source localization problem [8], [9]. Our approach was based on an equivalent current dipole model for the source. We questioned the influence of the spatial distribution of the sensors and of the propagation model on the localization performance, as well as the robustness to noise. We provided experiments and validation on real SEEG recordings of epileptic spikes, a premiere in such invasive framework. The main conclusions we drawn is that better localization performance was achieved when choosing particular subset of sensors, while these performances decreased when considering the whole set of available sensors. Besides, the number of averaged time samples were shown to have also an influence on the localization accuracy. It then appears that a trade off is to be made between these factors (amount of sensors, sources to sensors distances and amount of time samples). In this paper, we provide novel experiments specifically addressing these questions both on simulation and on real recordings of epileptic spikes.

## II. SEEG FORWARD/INVERSE PROBLEM

### A. Forward problem

At each time instant, the general forward problem can be written as follows [2]:

$$\Phi = \mathbf{K} \cdot \mathbf{J} \quad (1)$$

$\mathbf{K} \in \mathbb{R}^{N_c \times (3N_s)}$  is the propagation model (lead field matrix), coding the distances and the propagation coefficients between the  $N_s$  sources and the  $N_c$  captors. Electrical potentials  $\Phi \in \mathbb{R}^{N_c \times 1}$  recorded by the  $N_c$  electrodes are generated by neural sources, usually modeled as equivalent current dipoles  $\mathbf{J} \in \mathbb{R}^{(3N_s) \times 1}$  (considering their projections in Cartesian coordinates). The propagation of the sources on the sensors is assumed to be instantaneous, thus resulting in a linear mixing of the sources in  $\Phi$ . We suppose that the recorded potentials can be fully explained by the physiological activities in  $\mathbf{J}$ , no additive noise is then considered<sup>1</sup>.

<sup>1</sup>In the present paper, we assume that the potential of the common reference electrode is 0. The non-null reference problem is addressed by [10], [11] for scalp EEG and by [12], [13] for SEEG recordings.

<sup>1</sup> All authors are with the Université de Lorraine, CRAN, UMR 7039, 54500 Vandoeuvre les Nancy, France and with the CNRS, CRAN, UMR 7039, France [steven.le-cam@univ-lorraine.fr](mailto:steven.le-cam@univ-lorraine.fr)

<sup>2</sup> Louis Maillard is also with the CHU Nancy, Neurology Service, 54000 Nancy, France [l.maillard@chu-nancy.fr](mailto:l.maillard@chu-nancy.fr)

The authors thank Prof. S. Colnat-Coulbois (Nancy) for the neurosurgical contributions and the ANR SEPICOT for funding

The accuracy of the forward problem written in (1) greatly depends on the propagation model  $\mathbf{K}$ . Finite element models (FEM) approximate the volume conduction through a discretization of the brain medium. In our simulation, we have generated a five compartments FEM model: gray matter, white matter, cerebrospinal fluid, bone and scalp. The conductivities were chosen constant for a given tissue, regardless of the orientation ( $0.33S/m$  for the gray matter,  $0.2S/m$  for the white matter,  $0.33S/m$  for the scalp and  $0.004S/m$  for the skull bones [14]). More details on our FEM computation can be found in [9].

### B. Inverse problem

The inverse problem aims at estimating the source parameters from the measurements based on a given propagation model. FEM provide high modeling accuracy but is highly computationally demanding. In previous works [8], [9], we demonstrated that a simple analytical model like the One-Sphere Model (OSM) provide a satisfactory approximation of the inner brain volume conduction. The OSM is based on an assumption of homogeneity and isotropy inside the sphere, and remains analytically tractable [15]. In practice, the brain volume is fitted within a sphere roughly modeling the border between the skull and the brain, taking into account the high difference in conductivity at this frontier. This latter model has been used to perform the inversion task in this study.

Depending on how the sources are modeled, two classes of inverse problems can be distinguished [2], [4]. A first class of approaches use the so-called distributed source models, leading to a linear but severely ill-posed problem. The second class of methods (used in this paper) consists in considering only one (or few) dipole(s), resulting in an over-determined non-linear problem. In specific cases (ictal activities or interictal spikes for example), some brain regions (sources) are generating a signal having a much higher amplitude than the other regions. In this case, the recorded electrical activity can be indeed explained with one to few dipoles [1]. We focus here on the reconstruction of a single dominant dipole, leaving the multiple sources localization problem for a later study. Reconstructing a dipole implies estimating its 6 parameters, 3 for position and 3 for orientation and amplitude. Our goal is to enlighten the main factors impacting the SEEG-based dipole parameter estimation. Considering a single dipole, the mixing model of eq.(1) can be written as:

$$\Phi = \mathbf{k} \cdot \mathbf{j} + \mathbf{N} \quad (2)$$

where  $\mathbf{k}$  ( $N_c \times 3$ ) is the vector corresponding to the projection coefficients of the dominant source  $\mathbf{j}$  ( $3 \times 1$ ) on the  $N_c$  sensors.  $\mathbf{N}$  ( $N_c \times 1$ ) contains the projection of all the other sources on the electrodes, seen here as additive noise (from the main dipole point of view).

The algorithm we use for the inversion is the modified version of the fixed dipole approach [16], including a constrained optimization step (the solution is confined to the interior of the sphere fitting the brain) solved by sequential quadratic programming optimization [17], [18].

## III. SOLVING THE SEEG-BASED DIPOLE INVERSION

This section explains the rationale of this paper by addressing two main questions that have arisen in our previous studies: how the amount and the position of the sensors affects the localization results and which is the necessary number of time samples to be averaged.

### A. Which set of sensors is needed?

In [19], the influence of the amount of sensors on the localization results has been addressed in the context of scalp EEG (where the electrodes are covering the scalp homogeneously). The conclusion was that increasing the amount of sensors improves the localization. These results need be reconsidered in the SEEG context, where the quantity of used sensors seem not to be as preponderant as their particular positioning with regard to the location of the source. Usually, the SEEG setup consists in ten to fifteen electrodes, each of them being composed of a dozen of contacts. Up to 200 measuring contacts are then available. The electrodes insertion is done according to previous clinical hypothesis and is subject to anatomical constraints.

In previous works, we give some basic thoughts on undesirable sensor configurations [8]. In summary, at least 6 measurements are needed to retrieve the 6 components of a dipolar source. These 6 sensors have to fulfill simple geometrical constraints: they cannot be collinear, making irrelevant the use of a single electrode for localization purpose. Also, they have to lie in different planes. These precautions might be theoretically sufficient in ideal no-noise case. However, the effect of signal to noise ratio (SNR) has to be taken in considerations for realistic setup. In the independent white noise case [8], [9], increasing the number of sensors was shown to enhance the localization performance. Besides, we also put forward the hypothesis that a reliable localization was possible provided that a sensor is placed close enough to the source, as the SNR decreases on far sensors. This question is further explored in section IV-A on simulations.

### B. How many time samples are needed?

In real application, a common technique to improve the SNR is to average similar patterns (in general spikes or evoked potentials) over several trials. The resulting position stands for an averaged localization over the considered trials. The effect of the averaging has been studied in [20] for surface EEG dipole localization. It is shown that using a large amount of time samples (from 10 up to 100) helps in delineating the cortical epileptogenic lesion or the irritative zone. If the activity of interest is not correlated with the noise, a high SNR can indeed be obtained in the whole head volume by averaging and the whole set of SEEG sensors might be used with confidence. However, when the number of available (and validated) time samples is low, the sensors distant from the source are likely to exhibit critically low SNR. Thus, as demonstrated in [9] on real epileptic spikes, it might be more adequate to consider only a sufficient amount of close sensors with high SNR. In the result section IV-A, we deepen the analysis addressed in [9] by considering the

cross effect of the chosen subset of sensors with the number of time samples considered in the averaging.

#### IV. APPLICATION

##### A. Simulation

In order to evaluate the influence of the sensors to source distance, we conducted the following simulations (under Matlab): a standard head volume (without anatomical malformation) has been chosen, in which the implantation of 12 SEEG electrodes has been simulated, 9 electrodes being positioned in the right hemisphere and 3 electrodes in the left one (this SEEG setup is inspired from common schemes performed in temporal lobe epilepsy context). Each electrode consists in 7 to 10 equally spaced contacts inside the brain. The amount of sensors is of 112, 86 in the right hemisphere and 26 in the left hemisphere. This simulated setup is given on fig. 1. The potential on the sensors are simulated using a realistic FEM lead-field matrix (see section II-A).

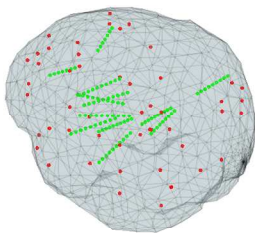


Fig. 1. Simulated setup: 112 SEEG contacts on 12 electrodes (green) and 50 dipoles (red)

Using this head setup, we successively placed dipolar sources on a regular 3D grid having 9mm between points. For computational reasons, we considered only a subset of 50 dipoles placed within the segmented gray matter, covering the whole brain volume. For each position, the three orthogonal orientations ( $O_x$ : inion-nasion,  $O_y$ : right-left and  $O_z$ : bottom-up) are considered. Thus  $3 \times 50 = 150$  dipoles configuration to be retrieved.

The presence of additive white noise has been simulated. We propose two different noise level, computed from the mean power of the whole 112 simulated potential on the sensors, due to all the 150 simulated dipoles. More precisely,  $\sigma_1 = M_p/10$  and  $\sigma_2 = M_p/\sqrt{2}$  (i.e., a noise attenuated by 20dB, respectively 3dB, with respect to  $M_p$ ), where

$$M_p = \frac{1}{M \cdot D} \sum_{d=1}^D \sum_{m=1}^M |V_{dm}|, \quad (3)$$

is the mean magnitude of the potentials  $V_{dm}$  (generated by dipole  $d$  on electrode  $m$ ) over the whole set of  $M = 112$  sensors and the  $D = 3 \times 50$  dipoles. Roughly speaking, the  $\sigma_1$  noise level corresponds to a source visible almost all over the brain (e.g. after averaging on several time instants), while the  $\sigma_2$  noise models a source mainly visible on close electrodes (e.g. few instants available for averaging). For each noise level, we have computed 100 noise realizations.

We performed the localization using all the available 112 sensors, using the dipole fitting procedure described in

section II-B. On figure 2, the mean position error for each 50 dipoles (over the 3 orientations and 100 noise realizations) is given as a function of their respective distance with the closest sensor (dashed and dotted curves). These results are obtained in a particular head volume, with an OSM lead-field based on a fixed fitted sphere, and with a particular SEEG setup. For this reason, commenting each particular values is useless, and we rather consider the trend of the position error vs distances to sensors. These curves are represented as bold lines computed using a cubic interpolation of the data sets. For both noise levels, it can be observed that when a sensor is close enough from the source (i.e. below 2.8cm for  $\sigma_1$  and 1.5cm for  $\sigma_2$ ), the error position remains satisfactory (i.e. below 1cm), whatever its particular position in the brain volume. For the dipoles that overpass these distance limits, several reasons can be put forward to explain the poor localization results, such as a critically low SNR, or their proximity with the head frontier where the quality of the used propagation model (OSM) can be questionable [9].

Still, white noise do not provide a realist modeling of the additive physiological noise  $\mathbf{N}$  (see eq.(2)). On the other hand, simulating the above single dipole scheme with different scenarios of correlated nuisance is not relevant, because of the huge amount of possible configurations qualitatively different from each other. Instead, we present in the next section an experiment on real epileptic spikes, which we believed will provide more convincing results. On these data, we evaluate the cross influence of the subset of sensors with the time averaging procedure.

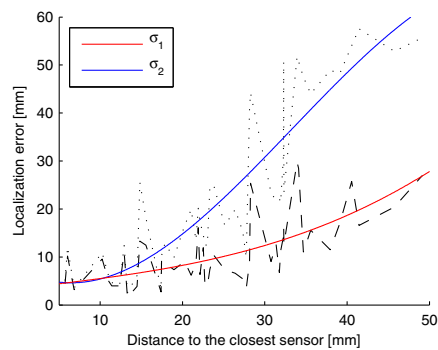


Fig. 2. Dipole localization error vs distance to the closest sensor. See text for explanations.

##### B. Real epileptic spikes

We analyze in this study the SEEG recordings of a 28 year-old woman with drug-resistant left insulo-opercular epilepsy. She gave her informed consent prior to participation. Ten depth electrodes were implanted in the left hemisphere, driven by the presurgical investigation. On the depth electrode R' (middle insula/central operculum), interictal epileptic spikes were clearly identified by trained neurophysiologists, with high signal to noise ratio and a presumably focal localization, i.e., the absence of other co-activated epileptic sources. Time averaging was performed using the following procedure: the signal from the R'6

contact (presenting highest amplitude spikes, thus assumed to be the position of the source) was high-pass filtered. Twenty spikes were then selected by thresholding and confirmed by a trained electrophysiologist. For each peak, the time instant of its highest value was retained. We then select, on each sensor,  $k = [1, 2, 3, 5, 7, 10, 15, 19, 20]$  among the 20 instants and average their corresponding recorded potentials. The localization is next performed using these averaged potentials. In order to have reliable results, localization was performed on 100 random combinations of  $k$  among 20 and the localization errors were averaged (except of course for  $k = 1$  or  $k = 19$ , when only 20 combinations are possible, and for the single combination for  $k = 20$ ). These results (localization error with respect to sensor R'6) are presented figure 3.

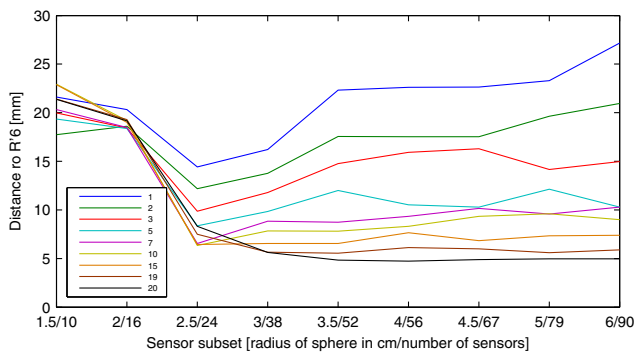


Fig. 3. Estimated position (distance to R'6) vs subset of sensors. Each curve represents a given amount of averaged spikes (mean of 100 subaverages).

In order to evaluate the cross influence of the time averaging with the used sensor configuration, we considered 10 different sensor subsets, depending on the distance of the sensors to R'6. The first configuration contains the 10 closest sensors, those within a sphere of radius 1.5cm centered in R'6. We then increase the radius by steps of 5mm to define the next configurations, increasing thus the number of used sensors, until including the whole set. Figure 3 shows the distance of the estimated dipole to R'6 with respect to the used sensor subsets, for each amount of averaged spikes (after averaging over their respective 100 subaverages). The results point out that a minimum amount of sensors with good spatial disparity is needed. In this experiment, the 16 sensors situated below 2cm from R'6 belong to two parallel electrodes, explaining the bad localization results. It is straightforward to see that increasing the number of spikes in the averaging indeed enhance the SNR, and thus the localization accuracy. When enough spikes are considered, (10 in this example), the localization is robust to the inclusion of additional sensors in the subset. But when the number of available spikes is low for averaging, the results point out that an adequate sensor configuration close to the source has to be chosen. In this particular experiment, a good trade-off (localization error below 1cm) is obtained by averaging 5 to 10 spikes on a subset of 24 sensors within a radius of 2.5cm.

## V. CONCLUSION

We evaluate the influence of the sensors subset and of the averaging on the dipolar localization accuracy in the intracerebral SEEG context. The results point out the need of a selection strategy of the adequate SEEG sensors subset to be considered in the localization process, depending on the SNR and on the number of time points available for averaging. Based on these conclusions, we plan to address the multiple dipole localization problem in future work, by iteratively determining for each dipole to localize an adequate selection of surrounding sensors.

## REFERENCES

- [1] L. Koessler, *et al.*, "Source localization of ictal epileptic activity investigated by high resolution EEG and validated by SEEG," *Neuroimage*, vol. 51, no. 2, pp. 642–653, 2010.
- [2] S. Baillet, J. C. Mosher, and R. M. Leahy, "Electromagnetic brain mapping," *Signal Processing Magazine, IEEE*, vol. 18, no. 6, pp. 14–30, 2001.
- [3] C. M. Michel, *et al.*, "EEG source imaging," *Clinical neurophysiology*, vol. 115, no. 10, pp. 2195–2222, 2004.
- [4] A. van Oosterom, "The inverse problem of bioelectricity: an evaluation," *Medical & biological engineering & computing*, vol. 50, no. 9, pp. 891–902, 2012.
- [5] B. Yvert, *et al.*, "Localization of human supratemporal auditory areas from intracerebral auditory evoked potentials using distributed source models," *Neuroimage*, vol. 28, no. 1, pp. 140–153, 2005.
- [6] N. Chang, R. Gulrajani, and J. Gotman, "Dipole localization using simulated intracerebral EEG," *Clinical neurophysiology*, vol. 116, no. 11, pp. 2707–2716, 2005.
- [7] N. von Ellenrieder, L. Beltrachini, and C. H. Muravchik, "Electrode and brain modeling in stereo-EEG," *Clinical Neurophysiology*, vol. 123, no. 9, pp. 1745–1754, 2012.
- [8] V. Caune, *et al.*, "Dipolar source localization from intracerebral SEEG recordings," in *Engineering in Medicine and Biology Society (EMBC), 2013 35th Annual International Conference of the IEEE*. IEEE, 2013, pp. 41–44.
- [9] —, "Evaluating dipolar source localization feasibility from intracerebral seeg recordings." *NeuroImage*, 2014. [Online]. Available: <http://www.sciencedirect.com/science/article/pii/S1053811914003383>
- [10] R. D. Pascual-Marqui, "Discrete, 3D distributed, linear imaging methods of electric neuronal activity. part 1: exact, zero error localization," *arXiv preprint arXiv:0710.3341*, 2007.
- [11] D. Yao, "A method to standardize a reference of scalp EEG recordings to a point at infinity," *Physiological measurement*, vol. 22, no. 4, p. 693, 2001.
- [12] R. Ranta, R. Salido-Ruiz, and V. Louis-Dorr, "Reference estimation in EEG recordings," in *Engineering in Medicine and Biology Society (EMBC), 2010 Annual International Conference of the IEEE*. IEEE, 2010, pp. 5371–5374.
- [13] N. Madhu, *et al.*, "A unified treatment of the reference estimation problem in depth EEG recordings," *Medical & biological engineering & computing*, vol. 50, no. 10, pp. 1003–1015, 2012.
- [14] L. Geddes and L. Baker, "The specific resistance of biological material: a compendium of data for the biomedical engineer and physiologist," *Medical and biological engineering*, vol. 5, no. 3, pp. 271–293, 1967.
- [15] D. Yao, "Electric potential produced by a dipole in a homogeneous conducting sphere," *IEEE transactions on bio-medical engineering*, vol. 47, no. 7, pp. 964–966, 2000.
- [16] M. Scherg, "Fundamentals of dipole source potential analysis," *Auditory evoked magnetic fields and electric potentials. Advances in audiology*, vol. 6, pp. 40–69, 1990.
- [17] *Optimization Toolbox Users Guide*. Mathworks®, 2014.
- [18] R. Fletcher, *Practical methods of optimization*. Wiley, 2013.
- [19] G. Lantz, *et al.*, "Epileptic source localization with high density EEG: how many electrodes are needed?" *Clinical Neurophysiology*, vol. 114, no. 1, pp. 63–69, 2003.
- [20] T. Bast, *et al.*, "Noninvasive source localization of interictal EEG spikes: effects of signal-to-noise ratio and averaging," *Journal of clinical neurophysiology*, vol. 23, no. 6, pp. 487–497, 2006.